



## Scholars Research Library

Archives of Applied Science Research, 2010, 2 (4): 111-118

(<http://scholarsresearchlibrary.com/archive.html>)



ISSN 0975-508X

CODEN (USA) AASRC9

## Growth and characterization of a promising ferroelectric relaxor material

R. Priya<sup>1</sup>, G. Bhagavannarayana<sup>2</sup>, S. Krishnan<sup>3</sup> and S. Jerome Das<sup>4,\*</sup>

<sup>1</sup>Department of Physics, R.M.D.Engineering College, R.S.M.Nagar, Kavaraipettai

<sup>2</sup>CGC Section, National Physical Laboratory, New Delhi, India

<sup>3</sup>Department of Physics, R.M.K.Engineering College, R. S. M. Nagar, Kavaraipettai

<sup>4</sup>Department of Physics Loyola College, Nungambakkam, Chennai

### ABSTRACT

Optical single crystals of ferroelectric trimethylammonium pentachloro barium dihydrate material were successfully grown by slow evaporation technique to a size of 20 X 17 X 3 mm<sup>3</sup> within a period of 4 weeks. The crystal was subjected to single crystal X-ray diffraction, UV-Vis analysis, mechanical and dielectric studies. HR-XRD studies were made to confirm the quality of grown crystal. The crystal show ferroelectric relaxor behaviour near curie temperature. The band gap energy and activation energy were also calculated. The relaxation rate is plotted with temperature to calculate activation energy and compared with the activation energy calculated from dc conductivity. It is found to be approximately equal.

**Key words:** Ferroelectric material, solution growth, Phase transition, band gap energy.

### INTRODUCTION

A<sub>2</sub>BX<sub>4</sub> where A = K, NH<sub>4</sub>, Rb, Cs, Na, N(CH<sub>3</sub>)<sub>4</sub>; B = Cu, Cd, Co, Zn; X = Cl, Br, I and A<sub>3</sub>BX<sub>5</sub>.2H<sub>2</sub>O where A = Na, NH<sub>3</sub>; B = Ba, Al; X = Cl, Br crystals exhibit very unusual physical properties and also represent the largest known group of insulating crystals with structurally incommensurate phases[1,2]. These show varying stoichiometries. Up to date ferroelectricity or pyroelectricity has been reported in methylammonium compounds with inclusion of di, tri and pentavalent metals, such as, (CH<sub>3</sub>NH<sub>3</sub>)<sub>5</sub> Bi<sub>2</sub>Cl<sub>11</sub>[3], CH<sub>3</sub>NH<sub>3</sub> AlCl<sub>4</sub>[4], [NH(CH<sub>3</sub>)<sub>3</sub>]<sub>3</sub>Sb<sub>2</sub>Cl<sub>9</sub>[5] and CH<sub>3</sub>NH<sub>3</sub> HgCl<sub>3</sub>[6]. The structural phase transitions occurring in such ABX<sub>3</sub> type compounds [7,8] have also been reported. An incommensurate phase shows no true periodicity but have two unrelated periods [9]. Incommensurate phases are generally encountered in metal oxides, sulphides and other materials where point defects may occur. Successive phase transitions and ferroelectricity at low temperatures had been reported for [N(CH<sub>3</sub>)<sub>4</sub>]<sub>2</sub>MnBr<sub>4</sub> [10,11]. Bansal et al [12,13] have reported Raman scattering study on [NH<sub>4</sub>] CuCl<sub>4</sub>.2H<sub>2</sub>O crystals at low temperatures

and found that the parallel spatial ordering of  $\text{NH}_4$  tetrahedral occurs at low temperature and these  $\text{NH}_4$  groups are randomly distributed at room temperature. It is seen from the literature that the title compound was synthesized and FTIR, TG/DTA, DSC studies have been made [14]. In this paper, we report on the size, cell parameters obtained from single crystal XRD studies, mechanical studies, dielectric studies and UV analysis of the grown crystal. The phase transition obtained from DSC results is compared with dielectric studies. A detailed study on relaxor behaviour is also reported.

## MATERIALS AND METHODS

### 2.1. Experimental

Single crystals of the title compound  $[(\text{CH}_3\text{NH}_3)_3\text{BaCl}_5 \cdot 2\text{H}_2\text{O}]$  hereinafter called as MAC-Ba, were grown by slow evaporation technique with the starting materials as methylammonium chloride and barium chloride (Analar Grade) in the ratio of 3:1. Triple distilled water was used for the growth. Care was taken to minimize the thermal or mechanical disturbances to the solution. Good quality single crystals as in Fig.1 were obtained after frequent recrystallization and filtration. Large crystal of about  $20 \times 17 \times 3 \text{ mm}^3$  dimension was harvested successfully in about 4 weeks. The size of the crystal obtained in our attempt is much higher to that of the previously reported [14].

### 2.2. Characterization

Single crystal X-ray diffraction measurements are performed using ENRAF NONIUS CAD4 diffractometer. Carefully cut crystals of  $0.3 \times 0.2 \times 0.2 \text{ mm}^3$  dimension are used to measure the cell parameters and cell volume. In order to confirm the presence of the functional groups in the crystal lattice, FTIR spectra was recorded by KBr pellet technique using BRUKKER IFS 66V spectrometer in the wave number range  $400 - 4000 \text{ cm}^{-1}$ . Optical absorption spectrum of the grown crystal was recorded using DRS UV visible spectrometer in the wavelength range 200-2000 nm. Dielectric studies were performed using HIOKI 3532-50 LCR HITESTER meter to confirm the ferroelectric behavior of the title compound.

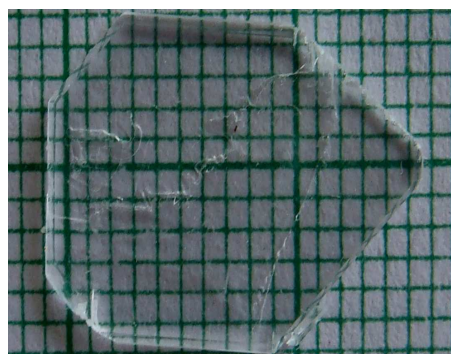


Figure 1 Photograph of the MAC-Ba crystal spectrum

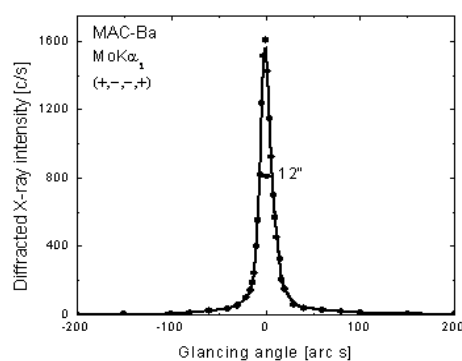


Figure 2 HR XRD

## RESULTS AND DISCUSSION

### 3.1 Single crystal XRD Analysis

The single crystal diffraction studies of the grown crystal were carried out and it is observed that MAC-Ba crystallizes in orthorhombic system. The cell parameters are  $a=6.721 \text{ \AA}$ ;  $b= 10.905 \text{ \AA}$ ;  $c= 7.120 \text{ \AA}$  which are different from both methylammonium chloride [15] and barium chloride dihydrate [16] showing the entry of the latter into the former material. Also, FTIR studies were made to identify the methyl groups and other bondings. The spectrum matches perfectly with that of already reported spectra of the title compound [14].

### 3.2 HR-XRD Studies

Fig.2 shows the high-resolution diffraction curve (DC) recorded for a typical MAC-Ba specimen using symmetrical Bragg geometry by employing the multicrystal X-ray diffractometer with  $\text{MoK}\alpha_1$  radiation. As seen in the figure, the DC is quite sharp without any satellite peaks which may otherwise be observed either due to internal structural grain boundaries or due to epitaxial layer which may sometimes form in crystals grown from solution [17]. The full width at half maximum (FWHM) of the diffraction curves is 12 arc sec, which is very close to that expected from the plane wave theory of dynamical X-ray diffraction [18]. The single sharp diffraction curve with very low FWHM indicates that the crystalline perfection is extremely good.

### 3.3 UV-Vis Spectral Studies

Single crystals are mainly used in optical applications where the optical transmission range and lower cutoff wavelength are very important. The UV-Vis absorption spectra shown in Fig.3 shows a lower cutoff wavelength of 270nm and the high transmittance in the entire visible region enables it to be a potential candidate for optoelectronic applications. A plot between  $h\nu$  and  $(\alpha h\nu)^2$  shown in Fig.4 is used to calculate the band gap energy and it is found to be 3.7eV.

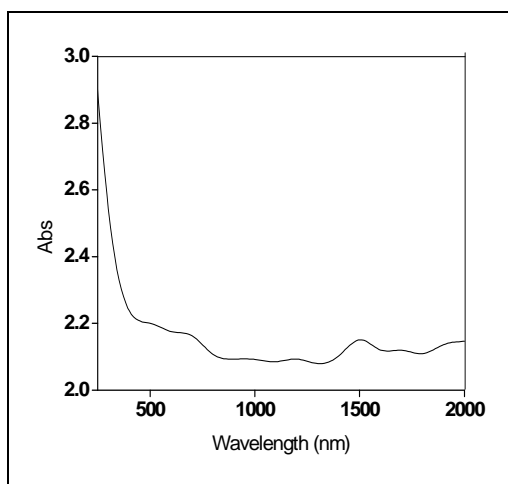


Figure 3 UV-Vis absorption spectrum

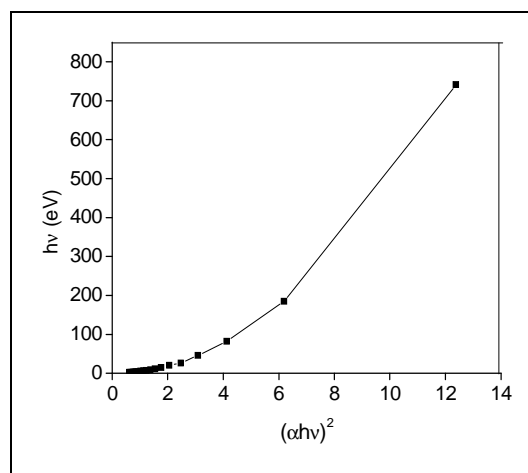


Figure 4 Variation of  $(\alpha h\nu)^2$  Vs  $h\nu$

### 3.4 Microhardness Studies

Microhardness of a crystal is its capacity to resist indentation. Physically hardness is the resistance offered by a material to the localized deformations caused by indentations [16]. This indentation hardness is measured as the ratio of the applied load to the surface area of the

indentation. In the present study, the indentations were carried out for loads P= 25-200g. For each load, several indentations were made and the average value of the diagonal length (d) was used to calculate the microhardness with the formula  $H_v = 1.8544 \frac{P}{d^2}$ . The hardness number ( $H_v$ ) increasing with the load (P) shows reverse indentation size effect (RISE) and a plot between the two is shown in Fig.5. A plot between log d and log P yields a straight line as shown in Fig.6 and the slope gives the work hardening coefficient (n) of the material which is calculated to be 2.499. According to Onitsch, the Meyer's index in the range of  $1.0 \leq n \leq 1.6$  is for hard materials and  $n > 1.6$  for soft materials [19]. Hence, it is inferred that MAC-Ba belongs to the soft category of materials.

According to Meyer's relation, the work hardening coefficient is related to the diagonal length by

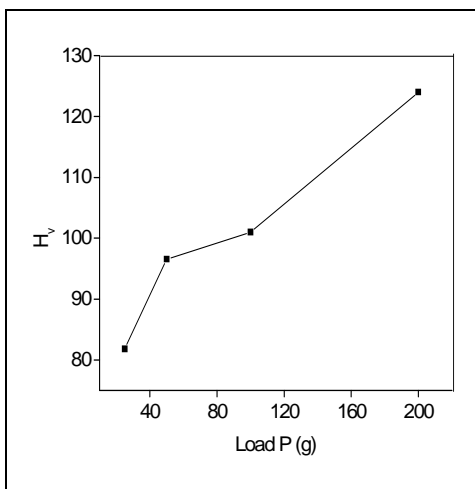


Figure 5 Load P Vs Hardness number  $H_v$

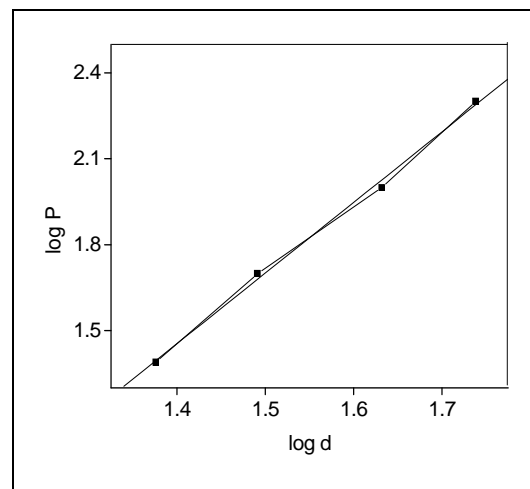


Figure 6 Log P Vs Log d

$$P = K_1 d^n \tag{1}$$

where  $K_1$  is an arbitrary constant obtained from a plot between load P and  $d^n$ . Since the material takes some time to revert to the elastic mode after every indentation, a correction x is applied to the d value and the Kick's law is related as

$$P = K_2 (d + x)^2 \tag{2}$$

From equation (1) & (2)

$$d^{\frac{n}{2}} = \left( \frac{K_2}{K_1} \right)^{\frac{1}{2}} d + \left( \frac{K_2}{K_1} \right) x \tag{3}$$

The slope calculated from a plot of  $d^{n/2}$  versus d yields  $(K_2/K_1)^{1/2}$  and the intercept is a measure of x. The fracture toughness ( $K_c$ ) is given by

$$K_c = \frac{P}{\beta C^{\frac{3}{2}}} \tag{4}$$

where C is the crack length measured from the centre of the indentation mark to the crack tip, P is the applied load and geometrical constant  $\beta = 7$  for Vickers’s indenter. The brittle index (B) is given by

$$B = \frac{H_v}{K_c} \tag{5}$$

The yield strength ( $\sigma_v$ ) of the material can be found out using the relation

$$\sigma_v = \frac{H_v}{2.9} \{1 - (n - 2)\} \left[ \frac{12.5(n - 2)}{1 - (n - 2)} \right]^{n-2} \tag{6}$$

The load dependent hardness parameters viz., work hardening coefficient(n), fracture toughness ( $K_c$ ), brittle index (B) and yield strength ( $\sigma_v$ ) are calculated for the MAC-Ba crystal and are given in Table.1

**Table.1 Microhardness data obtained on the MAC-Ba crystal**

Parameters	Values
Work Hardening coefficient (n)	2.449
Fracture Toughness ( $K_c$ ) ( $\text{kg/mm}^{3/2}$ )	3.035
Brittle index (B) ( $\text{m}^{-1/2}$ )	$3.323 \times 10^7$
Yield Strength ( $\sigma_v$ ) (MPa)	750.36

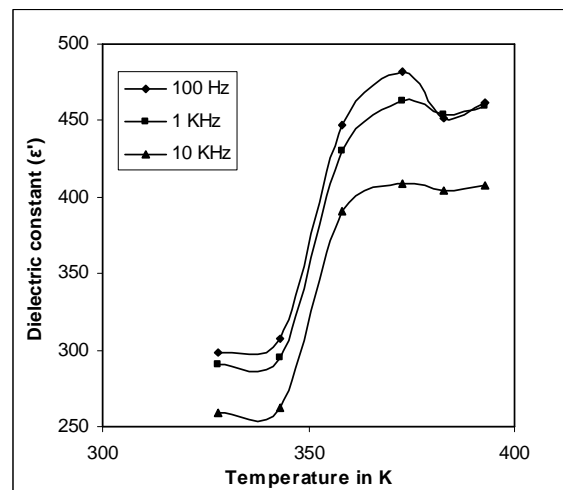


**Figure 7 Temperature Vs Dielectric Constant**

### 3.5 Dielectric Studies

The dielectric constant and the dielectric loss of MAC-Ba were measured in the frequency region from 50 Hz to 500 MHz. Fig.7 shows the variation of dielectric constant with temperature at different frequencies. The temperature dependence shows broad spectrum from which 101°C is reported [14] to be a phase transition from thermal studies. But this broad peak and the value of maximum dielectric constant ( $\epsilon'_{\max}$ ) decreasing with the frequency is the characteristic of relaxor behaviour. The high value of permittivity is also an evidence of relaxor behaviour.

Following Macedo et al [20], the real and imaginary parts of dielectric modulus are related to  $\epsilon'$  and  $\epsilon''$  as,

$$M^* = M' + iM'' \quad (8)$$

$$\text{where } M' = \frac{\epsilon'}{\epsilon'^2 + \epsilon''^2} \quad (9)$$

$$M'' = \frac{\epsilon''}{\epsilon'^2 + \epsilon''^2} \quad (10)$$

For a sample to exhibit relaxor behaviour, a plot of  $M''$  versus temperature should give a maximum at the temperature for which the dielectric relaxation frequency is equal to the measuring frequency. A plot between  $M''$  and temperature (T) also (not shown) indicates Debye-type relaxation behaviour [21].

Moreover, the imaginary part of dielectric modulus ( $M''$ ) plotted as a function of frequency at different temperatures as in Fig.8 shows dispersion of relaxation time. It is also understood from these two plots that measurements at frequencies less than 100 KHz is required in order to observe relaxation behaviour at a temperature less than 393 K. The relaxation time is defined as the inverse of angular frequency at the maximum of the  $M''$  ( $\omega\tau=1$ ).

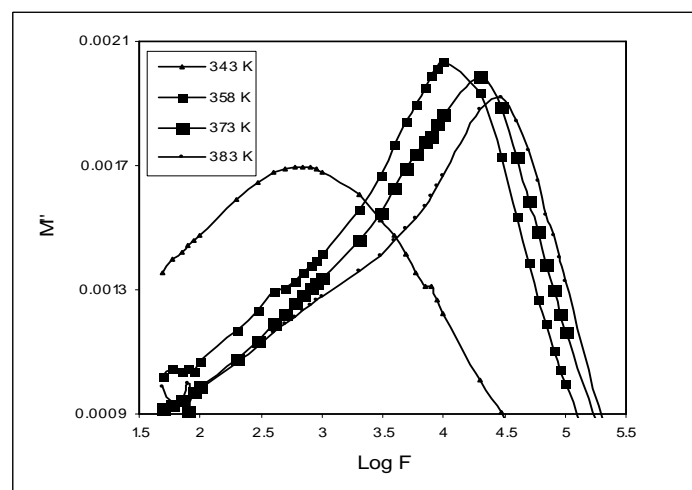


**Figure 8** Frequency Vs Imaginary part of dielectric modulus

A plot of relaxation rate ( $F_r$ ) vs  $1000/T$  is drawn and Arrhenius type of plot is obtained as shown in Fig.9. The activation energy is calculated to be 0.8 eV. This coincides approximately with the activation energy calculated from the plot between  $\log \sigma_{dc}$  and  $1000/T$  whose value is found to be  $E_a = 0.74$  eV.

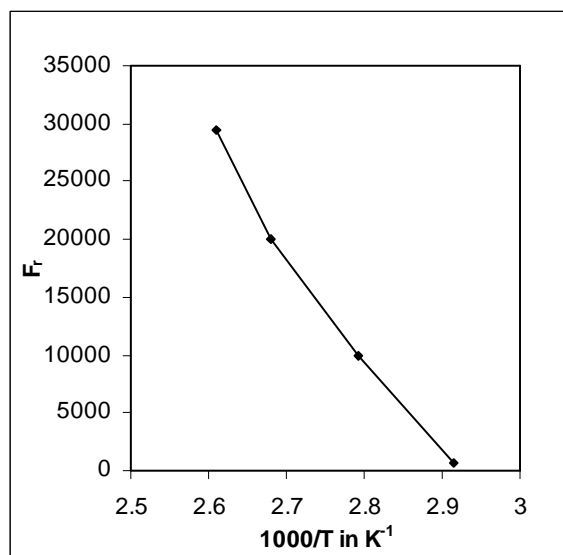


**Figure 9** 1000/T Vs Relaxation Rate( $F_r$ )

### CONCLUSION

MAC-Ba single crystals were grown by slow evaporation technique to a size of 20 X 17 X 3 mm<sup>3</sup>. The HR XRD studies were made to confirm that the grown crystal is defectfree. The UV cutoff wavelength was found to be 270nm. The bandgap energy  $E_g = 3.7$ eV was calculated from UV spectra. The mechanical hardness studies reveal that the work hardening coefficient of the title compound is 2.449 and hence it is concluded that it is a soft material. Temperature dependence of dielectric constant shows that  $\epsilon'$  increases with a higher rate above certain temperature indicating dipole polarization mechanism. The separate peaks observed in the frequency dependent  $M''$  in the temperature range 358K to 393K indicates a distribution of relaxation time and also reveals the presence of orientational polarization. This is caused due to hopping of charge carriers within the bulk. The values of activation energy deduced from dielectric relaxation are approximately equal to that obtained from dc conductivity measurements.

### Acknowledgement

The authors express their heartfelt gratitude to the facilities rendered by SAIF, IIT Madras, Chennai. One of the authors thanks the Management and Principal of R.M.D. Engineering College for their encouragements throughout the work. The support rendered Prof.S.Kalavathy and Ms.M.Joice Punitha, R.M.D.Engineering College and all our research colleagues is gratefully acknowledged.

---

**REFERENCES**

- [1] HZ Cummins, *Physics Reports*, **1990**, 185, 211.
- [2] JA Desilva, FEA Melo, JM Filho, FF Germano, JE Horeira, *J.Phys.C.Solid Stat. Phys.*, **1986**, 19, 3797.
- [3] J Mroz and R Jakubas, *Ferroelectric Lett.*, **1990**, 11, 53.
- [4] Z Czaplá, O Czupinski and Z Ciunik, *Solid State Commn.*, **1986**, 58, 383.
- [5] Maciej Bujak, Jacek Zaleski, *Crystal Engineering*, **2001**, 4, 241.
- [6] G Amirthaganesan, MA Kandhaswamy, V Srinivasan, *Indian J.Pure & App. Phys.*, **2003**, 41, 775.
- [7] Lisheng Chi, Ian Swainson, Lachlan Cranswick, Jae-Hyuk Her, Peter Stephens and Oswald Knop, *Journal of Solid State Chemistry*, **2005**, 178, 1376.
- [8] G Amirthaganesan, MA Kandhaswamy and M Dhandapani, *Cryst. Res. Technol.*, **2007**, 42, 684.
- [9] CNR Rao and J Gopalakrishnan, *Solid State Chemistry II Edition*, Cambridge University, Cambridge, **1977**.
- [10] Katsuhiko Hasebe, Takanao Asahi and Kazuo Gesi, *Acta Crys.*, **1990**, C46, 759.
- [11] Katsuhiko Hasebe and Takanao Asah, *Acta Crys.C45*, **1989**, 841.
- [12] ML Bansal, VC Sahni and AP Roy, *J.Phys.Chem.Solids*, **1979**, 40, 109.
- [13] AP Roy, VC Sahni and ML Bansal, *J.Phys.Chem.Solids*, **1979**, 40, 289.
- [14] G Amirthaganesan, MA Kandaswamy and V Srinivasan, *Cryst.Res.Technol.*, **2003**, 38, 908.
- [15] EW Hughe and WN Lipscomb, *J.Am.Chem.Soc.*, **1946**, 68, 1970.
- [16] BW Mott, *Microindentation hardness testing*, Butterworths, London, **1956**, 206.
- [17] G Bhagavannarayana, S Parthiban and Subbiah Meenakshisundaram, *J. Appl. Cryst.* **2006**, 39, 784.
- [18] BW Betterman and H Cole, *Rev. Mod. Phys.* 36, **1964**, 681.
- [19] EM Onitsch, *Mikroskopie*, **1947**, 2, 131.
- [20] PB.Macedo, CT Moynihan and R Bose, *J.Chem. Glasses*, **1972**, 13, 171.
- [21] KK Som, S Mollah, K Bose and BK Chaudhuri, *Phys.Rev. B* 47, **1993**, 534.